Geochemical Perspectives Letters

Siderophores and the formation of cerium anomalies in anoxic environments

D. Kraemer[1,2*], M. Bau[1]

OPEN ACCESS

https://doi.org/10.7185/geochemlet.2227

Abstract

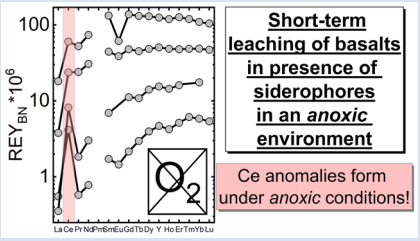

Microbes and plants affect the mobility of trace elements and may have done so since the onset of "life" on Earth. The recognition of such bio-effects on early Earth or Mars remains challenging and the impact of organisms on element mobilisation and redox cycling is largely unconstrained. Redox-sensitive trace elements, such as Ce, are used as geochemical proxies for reconstructing atmospheric oxygen levels, but bio-proxies are still largely lacking. We show that experimental water–rock interaction in presence of siderophores, globally abundant biogenic ligands excreted by microbes, fungi and plants, enhances lanthanoide mobilisation and produces positive Ce anomalies even under strictly anoxic conditions. This is the first evidence for bio-mediated oxidation of Ce and Ce anomaly formation in anoxic environments. Oxygen-independent fractionation of Ce from its redox-insensitive rare earth element neighbours during geo–bio interaction may hold the potential to use Ce anomalies as a bio-proxy in addition to its current use as a redox proxy.

Received 7 March 2022 | Accepted 3 July 2022 | Published 19 August 2022

Introduction

Cerium belongs to the lanthanoides, which, together with the pseudolanthanoid Y, are referred to as "rare earth elements and yttrium" (REY). The REY show coherent behaviour in the natural environment due to their similar charge and systematically decreasing ionic radii. Cerium is an exception, as it can be oxidised to Ce(IV) and hence decoupled from its redox-insensitive, strictly trivalent REY neighbors La and Pr. During pedogenesis and oxidative weathering, Ce(IV) may form insoluble cerianite (CeO_2) which remains fixed in the regolith when the REY(III) are gradually mobilised (Braun *et al.*, 1990), eventually producing Ce anomalies in normalised REY patterns of soil. Likewise, Fe and Mn-oxyhydroxides have the tendency to surface-oxidise Ce upon sorption, facilitating positive Ce_N anomalies at the mineral surfaces and, with time, progressively more negative anomalies in the associated (pore) solutions (Bau and Koschinsky, 2009). Due to their particle reactivity and the presumed immobility of REY, presence or absence of Ce anomalies in palaeoweathering profiles and marine chemical sediments are commonly used as a robust qualitative redox proxy (*e.g.*, German and Elderfield, 1990; Riding *et al.*, 2014).

Biota facilitates a strong control on redox-sensitive elements, such as Fe (*e.g.*, Byrne *et al.*, 2015). A class of biogenic ligands that interacts strongly with oxide and silicate minerals (Brantley *et al.*, 2001; Kraemer *et al.*, 2014) and that solubilises Fe, REY and other high field strength elements (Yoshida *et al.*, 2004; Christenson and Schijf, 2011; Bau *et al.*, 2013; Kraemer *et al.*, 2015, 2017) are the so-called "siderophores". These are excreted by bacteria, plants and fungi, primarily to mobilise bioessential Fe (Haas, 2003) and to cope with metal toxicity (Braud *et al.*, 2010). Siderophore-promoted oxidation of Ce under oxic conditions has been described in literature (Brantley *et al.*, 2001; Yoshida *et al.*, 2004; Bau *et al.*, 2013; Kraemer *et al.*, 2015, 2017).

This study fills the important knowledge gap on the impact of the oxygen level of a system on this process. The naturally abundant microbial siderophore desferrioxamine B (DFOB), produced by *Streptomyces pilosus*, and the fungal siderophore desferrichrome (DFC), produced by *Ustilago sphaerogena*, are used as model siderophores for batch incubation experiments with powdered igneous rocks to simulate water–rock interaction (WRI) at oxygen levels of (i) 0 ppmv O_2 ('anoxic'), (ii) 0.1 % O_2 ('hypoxic') and (iii) ~21 % O_2 (present atmospheric level; 'oxic'). The experiments were conducted at room temperature in a gloveless anaerobic chamber with various sampling times and a fixed rock/water ratio of 20 g/L.

Results

A set of igneous rocks, comprised of mid-ocean ridge basalt (MORB; glass and microcrystalline), island-arc basalt (IAB), andesite and granite, was chosen for investigating WRI at different atmospheric conditions. Concentrations of REY in leachates were normalised to those in the respective bulk rock (subscript "BN") to facilitate comparison between mobilised REY relative to the bulk rock inventory. We emphasise that the rock samples were pristine and that the bulk rock REY patterns (Fig. S-1) did not show any signs of alteration.

1. Department of Physics and Earth Sciences, Jacobs University Bremen, Campus Ring 1, 28759 Bremen, Germany
2. Current address: Federal Institute for Geosciences and Natural Resources (BGR), Stilleweg 2, 30655 Hannover, Germany
* Corresponding author (email: dennis.kraemer@bgr.de)

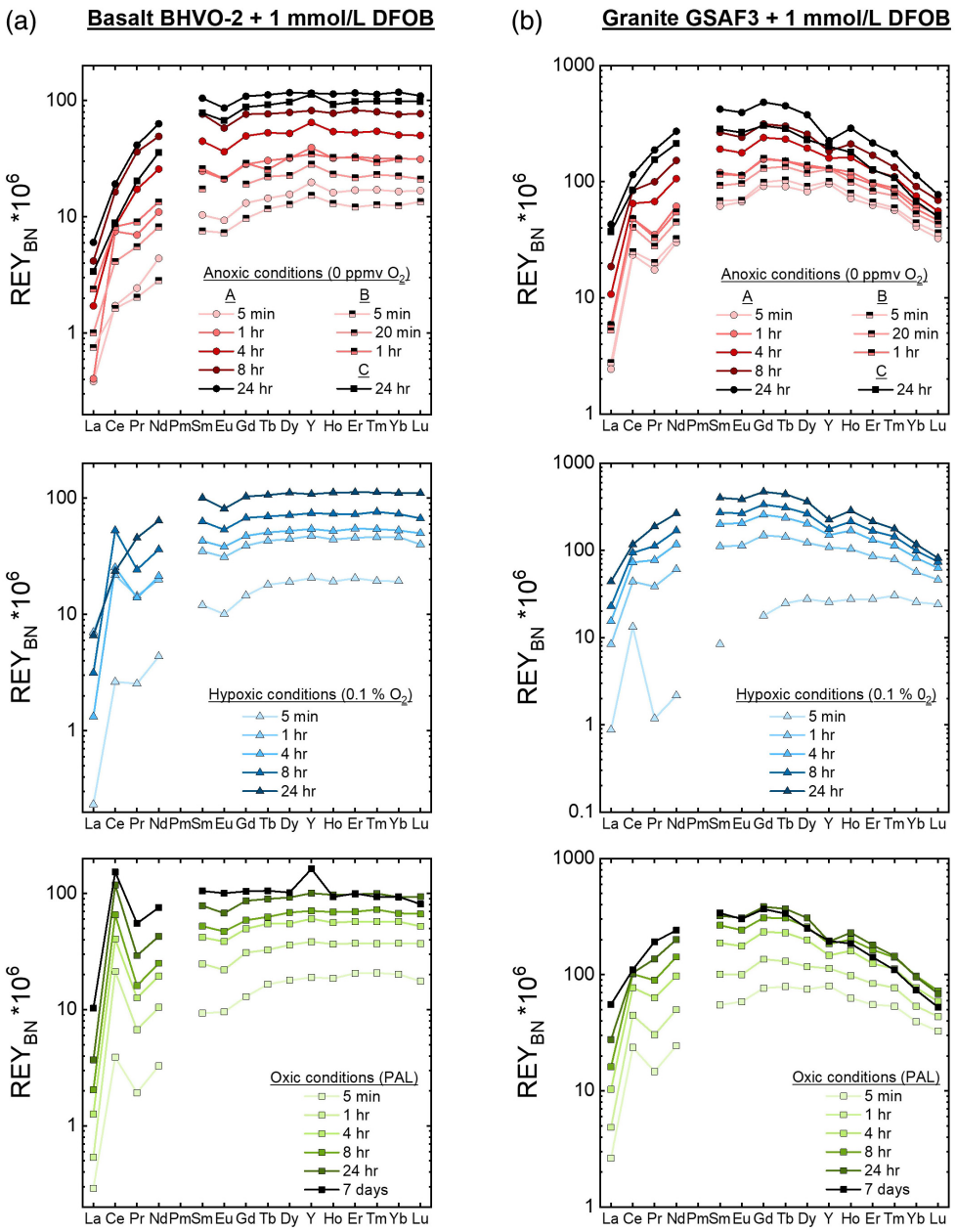

Figure 1 REY_{BN} patterns of time series experiments with **(a)** basalt and **(b)** granite.

Figures 1–3 show REY_{BN} patterns of the leaching experiments at different run times, and Figure 4 shows calculated Ce anomalies (Ce_{CN}/Ce_{CN}*) *vs.* Y/Ho ratio of the anoxic (shades of red, circles), hypoxic (shades of blue, triangles) and oxic experiments (shades of green, squares). Leaching of REY from igneous rocks in the presence of either of the two model siderophores under the three studied pO_2 conditions revealed the following:

(i) the amount of mobilised REY increases with time;

(ii) HREY mobilisation is stronger than LREY mobilisation, especially La is depleted;

(iii) patterns of the anoxic to oxic experiments at the same time interval are similar, except for Ce, and corroborate published data from oxic experiments (Kraemer *et al.*, 2015);

(iv) in the first 5 min of leaching, *positive* Ce_{BN} anomalies develop even under strictly anoxic conditions, regardless of mineralogical composition, texture and REY concentrations of the rock sample; after 60 min at the latest, these Ce_{BN} anomalies become smaller, and later disappear in all anoxic experiments, resulting in patterns *without* Ce_{BN} anomaly after 24 hr;

(v) positive Ce_{BN} anomalies formed in all hypoxic and oxic experiments after at least 5 min, except in experiments with glassy MORB and granite. Nevertheless, the Ce_{BN} anomalies that formed during the hypoxic experiments are less pronounced than those that developed during the oxic experiments, suggesting that pO_2 exerts a control on the formation of Ce anomalies during WRI with siderophores;

(vi) Y-Ho fractionation was more pronounced in the anoxic experiments than in the other experiments (Fig. 4).

In the course of individual experiments, pH first decreased from 5.5 to <5, then increased and mostly remained in the range

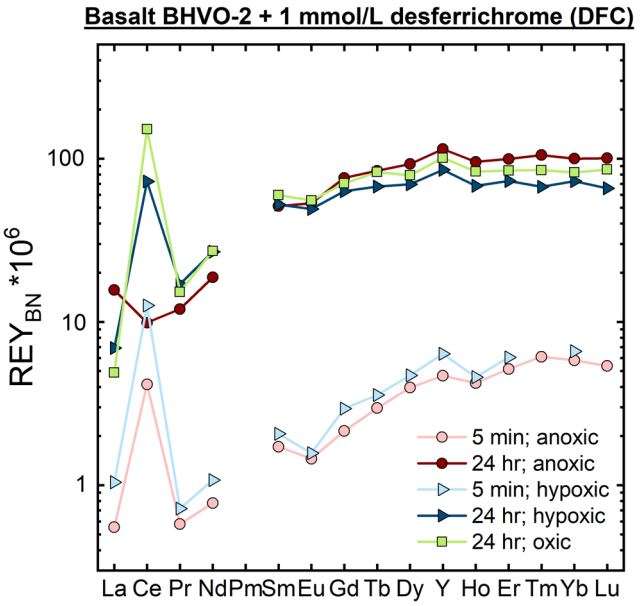

Figure 2 REY_{BN} patterns of experiments with basalt and DFC.

of 5–7 after 24 hr (Figs. S-2–S-4, Table S-4), similar to previous studies (Kraemer *et al.*, 2015). Some experiments reached pH values of 8 and higher. Cerium anomaly formation, especially under anoxic conditions, however, was not correlated with final solution pH (Figs. S-2, S-3). Leaching under anoxic and hypoxic conditions caused a generally slower pH increase over time (Fig. S-4). Over the observed pH range, DFOB speciation was dominated by H_4DFOB^+ species with minor to equal contributions of H_3DFOB (Fig. S-5).

Control experiments with DI and 0.01 mol/L HCl under anoxic conditions did not produce Ce anomalies in the leachate solutions (Fig. S-6).

Discussion

The experiments indicate that leaching of redox-insensitive REY(III) by both DFOB and DFC is largely independent of actual pO_2 as evidenced by very similar patterns between the individual experiments with the same run times. The patterns between the different experimental sets overlap, except for redox-sensitive Ce, implying that complexation of redox-insensitive trace elements with DFOB or DFC is solely a function of the complex stability constants, the mineralogical association of the REY, the texture of the rock, and the individual solubility of the host minerals, but *not* of oxygen. Due to the scarcity of available data for complexation of REY with DFC, the following discussion focuses on REY-DFOB interaction. Stability constants for REY-DFOB complexes are several orders of magnitude higher than those of mono- and dicarbonate REY complexes in seawater (Liu and Byrne, 1998), with log K_f of hexadentate complexes ranging from 10.09 for La to 15.19 for Lu at seawater ionic strength (Christenson and Schijf, 2011). In comparison, the hexadentate coordination of Fe^{3+} results in a stability constant of 30.6 (DFOB; Martell and Smith, 2001). The increasing complex stability from light to heavy REY is observed, *e.g.*, in the leachates of the basalts and andesites, as the patterns show an increase from $LREY_{BN}$ towards $MREY_{BN}$ and $HREY_{BN}$.

The only leachates with different REY_{BN} patterns are of glassy MORB (Fig. 3d; flat REY_{BN} without fractionation) and of granite (Fig. 1b; bell-shaped REY_{BN}). The "MREY bulge" observed in the granite experiment may be related to highly insoluble minerals present in felsic plutonic rocks. The leachates of glassy MORB show lower REY concentrations than those of the microcrystalline counterpart. As REY are incompatible with respect to most rock-forming igneous minerals, they are, in rocks with porphyritic/phaneritic textures, not incorporated into the crystal lattice but are preferentially located along grain boundaries and in the interstitial crystal spaces (Giese and Bau, 1994). During WRI, this REY pool is mobilised first since no dissolution of well-crystallised minerals is necessary. Divalent Eu is compatible with respect to, and incorporated into, Ca-rich plagioclase, and hence the REY pool on grain boundaries and in interstitial spaces is depleted in Eu (negative Eu_{CN} anomaly). When this pool is mobilised during WRI, the solution inherits the Eu_{CN} anomaly. In volcanic glass, however, Eu(II) and all REY(III) are homogenously distributed, and hence no Eu_{CN} anomaly can develop (Giese and Bau, 1994; Bach and Irber, 1998; Shibata *et al.*, 2006; Kraemer *et al.*, 2015).

We conclude that pO_2 neither influences the amount nor the fractionation of individual or total REY(III) mobilised from igneous rocks during WRI in the presence of DFOB or DFC. Our experiments demonstrate, in accordance with published data, that the solubilisation and complexation of isovalent REY with DFOB or DFC is oxygen independent.

Leaching under hypoxic and oxic conditions leads to only minor fractionation of the Y-Ho geochemical twins, but pronounced fractionation was observed during short-term WRI under anoxic conditions (Fig. 4). The stability constants of Y and Ho with DFOB are similar (Christenson and Schijf, 2011) and no significant fractionation would be expected, in contrast to our results. Yttrium, however, appears to have a higher initial accessibility during WRI than Ho (Bau *et al.*, 1998), which could explain the Y fractionation during short-term WRI.

Cerium oxidation by the siderophore DFOB under oxic conditions has been demonstrated in several studies. Yoshida *et al.* (2004) conducted adsorption experiments of REY-DFOB complexes on γ-Al_2O_3 and *P. fluorescens* and found that Ce behaves markedly different from La(III) and Pr(III). They demonstrated the presence of Ce(IV)-DFOB in solution and concluded an oxidation of Ce(III) to Ce(IV) during DFOB complexation/adsorption. Siderophore-mediated oxidation was also demonstrated during oxic WRI with igneous rocks (Bau *et al.*, 2013; Kraemer *et al.*, 2015) and during scavenging onto Mn (hydr)oxides (Kraemer *et al.*, 2017) with the development of a positive Ce_N anomaly.

In contrast to the log K_f of REY(III)-DFOB (between 10.09 ± 0.08 and 15.19 ± 0.02; Christenson and Schijf, 2011) and Ce(III)-DFOB hexadentate complexes (log $K_f \approx 11.59$; back-extrapolated from Nd(III)- and Pr(III)-DFOB data of Christenson and Schijf, 2011), log K_f of Ce(IV)-DFOB was estimated to be significantly higher (25–30; Yoshida *et al.*, 2004) and thus comparable to Fe(III)-DFOB. The DFOB-mediated oxidation of redox-sensitive elements under oxic conditions was explained as follows:

(i) a lowering of the oxidation potential by DFOB-complexation and rapid oxidation by ambient air ("air-oxidation"; Duckworth and Sposito, 2005) which increases the metal-ligand complex stability (Hernlem *et al.*, 1999; Kraemer *et al.*, 2014), and

(ii) a disequilibrium between Ce^{3+}_{aq} and Ce^{4+}_{aq} at the mineral–water interface, where minute amounts of tetravalent Ce in solution are strongly complexed by DFOB, facilitating further disequilibrium and Ce^{4+} regeneration by continuous oxidation of Ce^{3+} to maintain redox

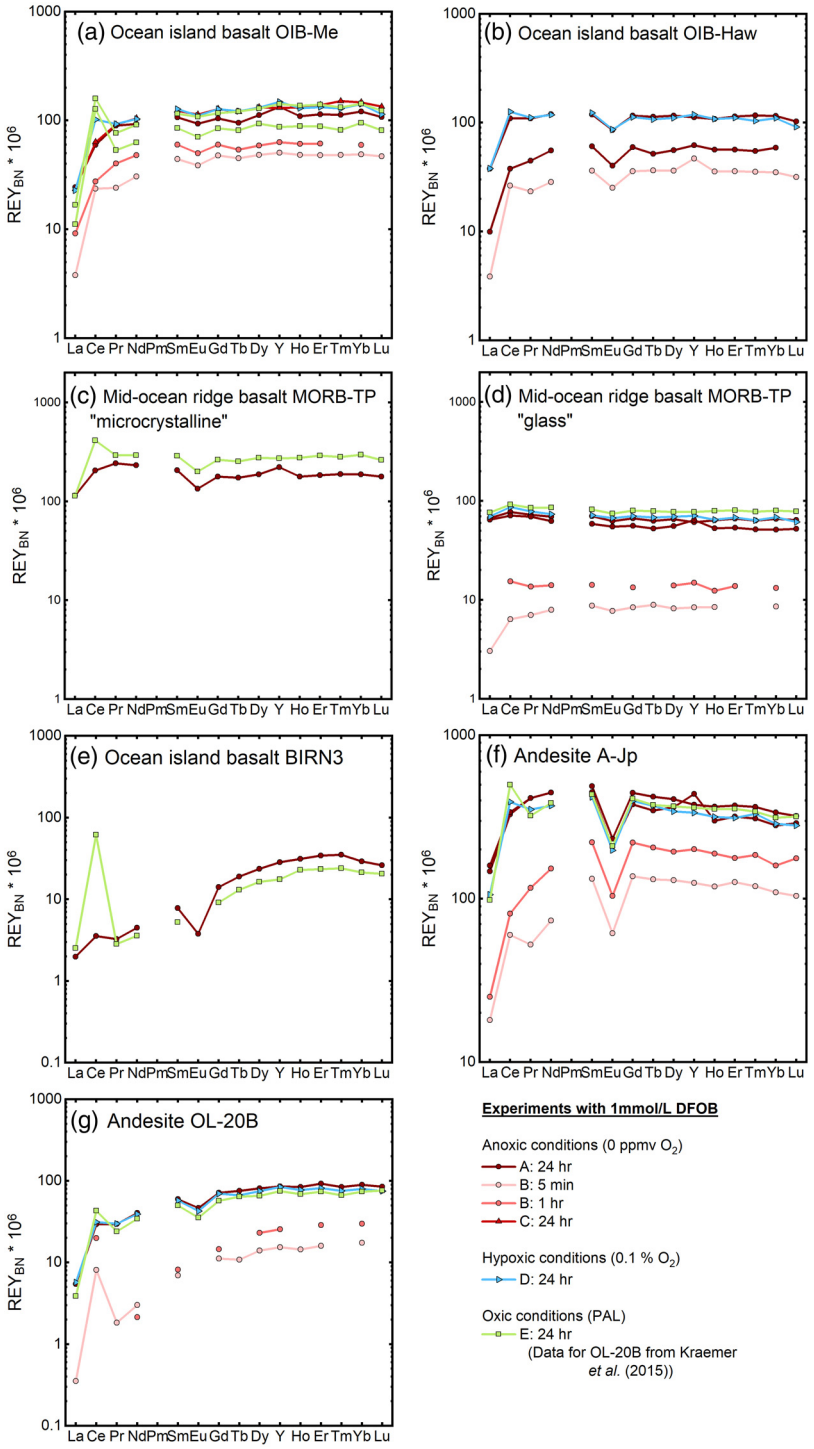

Figure 3 REY_{BN} patterns of leaching experiments with different igneous rocks. The letters A-E in the legend refer to different experiment runs. Details are listed in Table S-2.

equilibrium ("siderophore redox pump"; Bau *et al.*, 2013; Kraemer *et al.*, 2015, 2017).

Here, a Ce-LREY fractionation was observed even under anoxic conditions, although confined to short-term WRI. Clearly, the mechanisms proposed for Ce oxidation under (hyp)oxic conditions fail to explain this observation.

At the observed pH range, H_4DFOB^+ is the dominant species in solution, and anoxic Ce oxidation may follow a reaction path similar to the *anoxic siderophore-promoted oxidation* of ferrous Fe (Farkas *et al.*, 2001). The proposed reaction may be rewritten for a postulated anoxic Ce^{3+} oxidation process:

$$2\ Ce^{3+} + 3\ H_4DFOB^+ \rightarrow 2[Ce(IV)(HDFOB)]^{2+} + H_3DFOBmonoamide^+ + H_2O + 4\ H^+$$

The results show that Ce fractionation under anoxic conditions is limited to short-term WRI. Apparently, only "free" DFOB

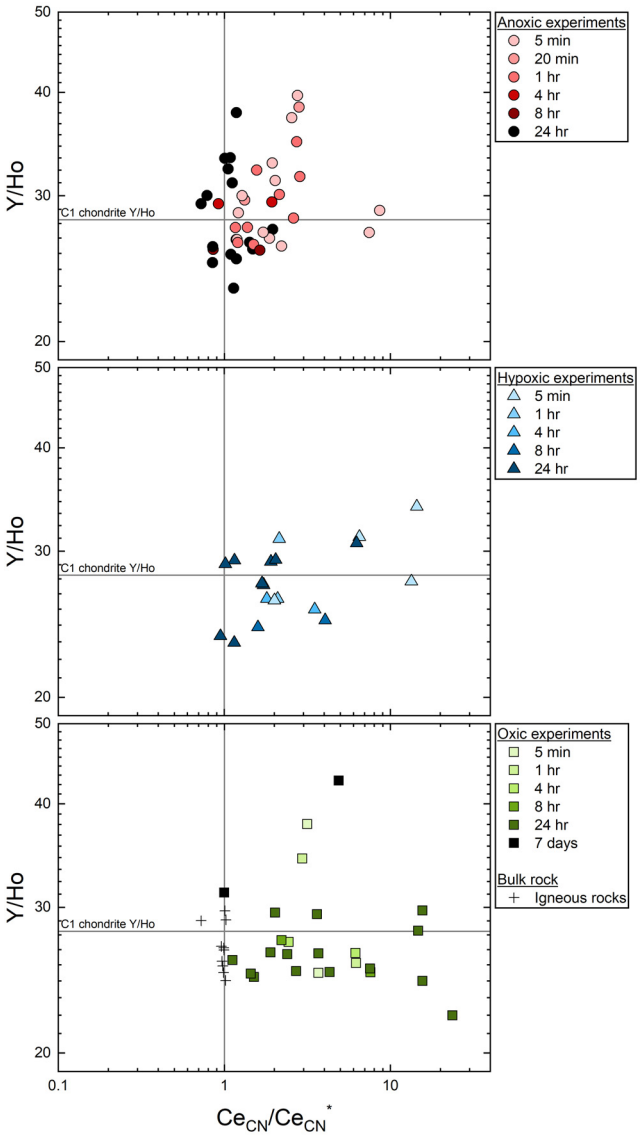

Figure 4 Graph of Ce_{CN}/Ce_{CN}* *vs*. Y/Ho ratio for bulk rocks and leachates.

molecules may participate in this redox reaction. Hence, this process is limited to the first minutes of leaching, when the activity of "free" H_4DFOB^+ is high and complexation with other metals with high complex stability (in particular Fe, which is present in excessive amounts in igneous rocks and which was also mobilised during the experiments; Figs. S-7–S-9, Table S-4) had not yet reduced the initial availability of this ligand. As WRI proceeds, the minute amounts of Ce(IV)-DFOB complexes formed under anoxic conditions are concealed by continuously increasing amounts of LREY(III)-DFOB complexes (including Ce(III)-DFOB) which effectively hide the Ce(IV) compounds in the REY_{BN} patterns.

We showed experimentally that complexation by biogenic ligands such as DFOB/DFC provides an *anoxic* and *hypoxic* pathway for the oxidation of Ce^{3+}, the subsequent oxidative decoupling of Ce from its neighbours in the REY series, and eventually the formation of positive Ce anomalies in normalised REY patterns of solutions produced during low-temperature WRI. We emphasise, however, that features of the Ce anomalies (*e.g.*, height of peak or relative fractionation from Pr(III) or Nd(III)), cannot be used to distinguish between redox-driven and siderophore-driven fractionation.

In modern seawater, complexation of bioessential micronutrients (*e.g.*, Fe(III)) is dominated by organic ligands, and previous studies have suggested that this ligand pool is dominated by siderophores (van den Berg, 1995; Gledhill *et al.*, 1998; Mawji *et al.*, 2008). Recent literature suggests that cyanobacteria may have produced siderophores for Fe(III) acquisition even before the Great Oxidation Event in the Palaeoproterozoic (Enzingmüller-Bleyl *et al.*, 2021). Today, siderophores also enable microorganisms to reduce toxic metal accumulation and to increase metal tolerance (*e.g.*, Braud *et al.*, 2010), which might have been evolutionary advantageous also for early life. Neaman *et al.* (2005) argued that organisms have had to cope with low nutrient bioavailability since at least the colonisation of the land surface. In (modern) soils, siderophores are at least as abundant as in marine systems, with concentrations up to the mmol/L range (Nelson *et al.*, 1988), and significantly enhance the mobility of trace elements such as REY (Wiche *et al.*, 2017). More than 500 different natural siderophore compounds have been described from natural systems (Boukhalfa and Crumbliss, 2002); yet to date, it is not possible to estimate abundances of organic ligands during early periods of Earth's history. In this regard, biosignatures may represent an important, yet unprecise tool.

As the different rock types showed very different REY fractionation patterns in the leachates, it is difficult to constrain REY patterns that are typical for WRI in presence of siderophores. The only distinct feature, apart from the Ce anomaly, is the occasionally very strong depletion of La (Bau *et al.*, 2013; Kraemer *et al.*, 2015, 2017; this study). Wang *et al.* (2020) identified La anomalies as fingerprints for methanotrophic activity. Therefore, we hypothesise that the observed La fractionation may also represent a characteristic biosignature of the involvement of siderophores in geochemical processes during WRI.

The fractionation of Ce in the presence of biomolecules as reported here sheds new light on the application of Ce anomalies as a geochemical proxy. Besides its well-established application as a qualitative redox proxy, Ce anomalies may have the potential to be used as a "bio-proxy", indicating the presence of (siderophore-producing) biota, potentially even under anoxic conditions.

While oxidation by bio-ligands will further complicate the use of geochemical redox proxies, this opens an exciting venue for future studies and potential applications, particularly in the field of astrobiology.

Acknowledgements

The very supportive editorial handling of Satish Myneni and the constructive comments of three anonymous reviewers are greatly appreciated. We acknowledge the financial support of the German Science Foundation (DFG) through grant KR4824/1-1 to D. Kraemer.

Editor: Satish Myneni

Additional Information

Supplementary Information accompanies this letter at https://www.geochemicalperspectivesletters.org/article2227.

Cite this letter as: Kraemer, D., Bau, M. (2022) Siderophores and the formation of cerium anomalies in anoxic environments. *Geochem. Persp. Let.* 22, 50–55. https://doi.org/10.7185/geochemlet.2227

References

Bach, W., Irber, W. (1998) Rare earth element mobility in the oceanic lower sheeted dyke complex: evidence from geochemical data and leaching experiments. *Chemical Geology* 151, 309–326. https://doi.org/10.1016/S0009-2541(98)00087-4

Bau, M., Koschinsky, A. (2009) Oxidative scavenging of cerium on hydrous Fe oxide: Evidence from the distribution of rare earth elements and yttrium between Fe oxides and Mn oxides in hydrogenetic ferromanganese crusts. *Geochemical Journal* 43, 37–47. https://doi.org/10.2343/geochemj.1.0005

Bau, M., Usui, A., Pracejus, B., Mita, N., Kanai, Y., Irber, W., Dulski, P. (1998) Geochemistry of low-temperature water-rock interaction: Evidence from natural waters, andesite, and iron-oxyhydroxide precipitates at Nishiki-numa iron-spring, Hokkaido, Japan. *Chemical Geology* 151, 293–307. https://doi.org/10.1016/S0009-2541(98)00086-2

Bau, M., Tepe, N., Mohwinkel, D. (2013) Siderophore-promoted transfer of rare earth elements and iron from volcanic ash into glacial meltwater, river and ocean water. *Earth and Planetary Science Letters* 364, 30–36. https://doi.org/10.1016/j.epsl.2013.01.002

Boukhalfa, H., Crumbliss, A.L. (2002) Chemical aspects of siderophore mediated iron transport. *Biometals* 15, 325–339. https://doi.org/10.1023/A:1020218608266

Brantley, S.L., Liermann, L., Bau, M., Wu, S. (2001) Uptake of Trace Metals and Rare Earth Elements from Hornblende by a Soil Bacterium. *Geomicrobiology Journal* 18, 37–61. https://doi.org/10.1080/01490450151079770

Braud, A., Geoffroy, V., Hoegy, F., Mislin, G.L.A., Schalk, I.J. (2010) Presence of the siderophores pyoverdine and pyochelin in the extracellular medium reduces toxic metal accumulation in *Pseudomonas aeruginosa* and increases bacterial metal tolerance. *Environmental Microbiology Reports* 2, 419–425. https://doi.org/10.1111/j.1758-2229.2009.00126.x

Braun, J.-J., Pagel, M., Muller, J.-P., Bilong, P., Michard, A., Guillet, B. (1990) Cerium anomalies in lateritic profiles. *Geochimica et Cosmochimica Acta* 54, 781–795. https://doi.org/10.1016/0016-7037(90)90373-S

Byrne, J.M., Klueglein, N., Pearce, C., Rosso, K.M., Appel, E., Kappler, A. (2015) Redox cycling of Fe(II) and Fe(III) in magnetite by Fe-metabolizing bacteria. *Science* 347, 1473–1476. https://doi.org/10.1126/science.aaa4834

Christenson, E.A., Schijf, J. (2011) Stability of YREE complexes with the trihydroxamate siderophore desferrioxamine B at seawater ionic strength. *Geochimica et Cosmochimica Acta* 75, 7047–7062. https://doi.org/10.1016/j.gca.2011.09.022

Duckworth, O.W., Sposito, G. (2005) Siderophore–Manganese (III) interactions. I. Air-Oxidation of Manganese(II) Promoted by Desferrioxamine B. *Environmental Science and Technology* 39, 6037–6044. https://doi.org/10.1021/es050275k

Enzingmüller-Bleyl, T.C., Boden, J.S., Herrmann, A.J., Ebel, K.W., Sánchez-Baracaldo, P., Frankenberg-Dinkel, N., Gehringer, M.M. (2021) Lack of Fe(II) transporters in basal Cyanobacteria complicates iron uptake in ferruginous Archean oceans. (Preprint) *bioRxiv*, 2021.11.08.467730. https://doi.org/10.1101/2021.11.08.467730

Farkas, E., Enyedy, E.A., Zékány, L., Deák, G. (2001) Interaction between iron(II) and hydroxamic acids: oxidation of iron(II) to iron(III) by desferrioxamine B under anaerobic conditions. *Journal of Inorganic Biochemistry* 83, 107–114. https://doi.org/10.1016/S0162-0134(00)00197-5

German, C.R., Elderfield, H. (1990) Application of the Ce anomaly as a paleoredox indicator: The ground rules. *Paleoceanography and Paleoclimatology* 5, 823–833. https://doi.org/10.1029/PA005i005p00823

Giese, U., Bau, M. (1994) Trace element accessibility in mid-ocean ridge and ocean island basalt: an experimental approach. *Goldschmidt Abstracts* 1994, 329–330. https://rruff.info/doclib/MinMag/Volume_58A/58A-1-329.pdf

Gledhill, M., van den Berg, C.M.G., Nolting, R.F., Timmermans, K.R. (1998) Variability in the speciation of iron in the northern North Sea. *Marine Chemistry* 59, 283–300. https://doi.org/10.1016/S0304-4203(97)00097-2

Haas, H. (2003) Molecular genetics of fungal siderophore biosynthesis and uptake: the role of siderophores in iron uptake and storage. *Applied Microbiology and Biotechnology* 62, 316–330. https://doi.org/10.1007/s00253-003-1335-2

Hernlem, B.J., Vane, L.M., Sayles, G.D. (1999) The application of siderophores for metal recovery and waste remediation: examination of correlations for prediction of metal affinities. *Water Research* 33, 951–960. https://doi.org/10.1016/S0043-1354(98)00293-0

Kraemer, D., Kopf, S., Bau, M. (2015) Oxidative mobilization of cerium and uranium and enhanced release of "immobile" high field strength elements from igneous rocks in the presence of the biogenic siderophore desferrioxamine B. *Geochimica et Cosmochimica Acta* 165, 263–279. https://doi.org/10.1016/j.gca.2015.05.046

Kraemer, D., Tepe, N., Pourret, O., Bau, M. (2017) Negative cerium anomalies in manganese (hydr)oxide precipitates due to cerium oxidation in the presence of dissolved siderophores. *Geochimica et Cosmochimica Acta* 196, 197–208. https://doi.org/10.1016/j.gca.2016.09.018

Kraemer, S.M., Duckworth, O.W., Harrington, J.M., Schenkeveld, W.D.C. (2014) Metallophores and Trace Metal Biogeochemistry. *Aquatic Geochemistry* 21, 159–195. https://doi.org/10.1007/s10498-014-9246-7

Liu, X., Byrne, R.H. (1998) Comprehensive Investigation of Yttrium and Rare Earth Element Complexation by Carbonate Ions Using ICP–Mass Spectrometry. *Journal of Solution Chemistry* 27, 803–815. https://doi.org/10.1023/A:1022677119835

Martell, A., Smith, R. (2001) *NIST Stability Constants of Metal Complexes Database 46, v. 6.0*. National Institute of Standards and Technology, Gaithersburg, MD.

Mawji, E., Gledhill, M., Milton, J.A., Tarran, G.A., Ussher, S., Thompson, A., Wolff, G.A., Worsfold, P.J., Achterberg, E.P. (2008) Hydroxamate Siderophores: Occurrence and Importance in the Atlantic Ocean. *Environmental Science & Technology* 42, 8675–8680. https://doi.org/10.1021/es801884r

Neaman, A., Chorover, J., Brantley, S.L. (2005) Implications of the evolution of organic acid moieties for basalt weathering over geological time. *American Journal of Science* 305, 147–185. https://doi.org/10.2475/ajs.305.2.147

Nelson, M., Cooper, C.R., Crowley, D.E., Reid, C.P.P., Szaniszlo, P.J. (1988) An *escherichia coli* bioassay of individual siderophores in soil. *Journal of Plant Nutrition* 11, 915–924. https://doi.org/10.1080/01904168809363856

Riding, R., Fralick, P., Liang, L. (2014) Identification of an Archean marine oxygen oasis. *Precambrian Research* 251, 232–237. https://doi.org/10.1016/j.precamres.2014.06.017

Shibata, S.-N., Tanaka, T., Yamamoto, K. (2006) Crystal structure control of the dissolution of rare earth elements in water-mineral interactions. *Geochemical Journal* 40, 437–446. https://doi.org/10.2343/geochemj.40.437

van den Berg, C.M.G. (1995) Evidence for organic complexation of iron in seawater. *Marine Chemistry* 50, 139–157. https://doi.org/10.1016/0304-4203(95)00032-M

Wang, X., Barrat, J.-A., Bayon, G., Chauvaud, L., Feng, D. (2020) Lanthanum anomalies as fingerprints of methanotrophy. *Geochemical Perspectives Letters* 14, 26–30. https://doi.org/10.7185/geochemlet.2019

Wiche, O., Tischler, D., Fauser, C., Lodemann, J., Heilmeier, H. (2017) Effects of citric acid and the siderophore desferrioxamine B (DFO-B) on the mobility of germanium and rare earth elements in soil and uptake in *Phalaris arundinacea*. *International Journal of Phytoremediation* 19, 746–754. https://doi.org/10.1080/15226514.2017.1284752

Yoshida, T., Ozaki, T., Ohnuki, T., Francis, A.J. (2004) Adsorption of rare earth elements by γ-Al_2O_3 and *Pseudomonas fluorescens* cells in the presence of desferrioxamine B: implication of siderophores for the Ce anomaly. *Chemical Geology* 212, 239–246. https://doi.org/10.1016/j.chemgeo.2004.08.046

Geochemical Perspectives Letters

Siderophores and the formation of cerium anomalies in anoxic environments

D. Kraemer, M. Bau

Supplementary Information

The Supplementary Information includes:

- Supplementary Methods and Samples
- Tables S-1 to S-4
- Figures S-1 to S-9

Supplementary Methods and Samples

Samples

A set of igneous rocks ranging in composition from mafic to felsic was chosen for investigating water-rock interaction (WRI) in presence of siderophores at various redox levels. In order to facilitate comparison, most of the incubation experiments were conducted on aliquots of rock powders also used in earlier experiments by Kraemer *et al.* (2015) for DFOB incubation experiments under atmospheric conditions. In addition, a Silurian island-arc basalt from the Dingle Peninsula, Ireland, and an intra-plate ocean-island basalt from Hawaii (BHVO-2, issued by the USGS as certified reference material) were used in the experiments. The igneous rocks were chosen to also represent different textures and plate-tectonic settings. The total set comprises two mid-ocean ridge basalts (MORB), four ocean island basalts (OIB), one island-arc basalt and one island-arc andesite, and an intraplate granite. The mineralogical composition of some of the rocks has been described by Kraemer *et al.* (2015) and is shown in Table S-1. The MORB sample was collected from an aphyritic sheet flow near the Turtle Pits hydrothermal field at the Mid-Atlantic Ridge (Haase *et al.*, 2007). The interior microcrystalline basalt (MORB-TP) and the exterior basaltic glass (MORB-TP glass) were sampled separately. OIB-Me is a primitive aphanitic alkali basalt from Mehetia Island (Society hotspot) and is discussed as sample Me90-05 by Binard *et al.* (1993). The second OIB sample, OIB-Haw, is a vesiculous tholeiite from Kilauea, Hawaii, and is also discussed by Giese and Bau (1994). The aphanitic island-arc basalt BIRN3 originates from the Clogher Head Formation of the Silurian Dunquin Group on the Dingle Peninsula, Ireland. Samples of more evolved mafic and intermediate composition are basaltic andesite OL-20b and andesite A-Jp. The basaltic andesite was originally described by Schnurr (1995) as a basaltic andesite originating from the Paleoproterozoic Ongeluk Formation of the Transvaal

Supergroup, South Africa. The island-arc andesite A-Jp originates from a lava flow underlying the Nishiki-numa spring (Hokkaido, Japan) (Bau *et al.*, 1998). The granite GSAF3 is from the Lebowa Granite Suite, Bushveld Complex, South Africa.
Concentration data (Table S-3) for the majority of the bulk rock samples and used herein for normalisation were taken from literature (Kraemer *et al.*, 2015).

Experimental
The leaching experiments (Table S-2) were done in multiple, independent batches named alphabetically from A to I. Batches labelled A-E, G, H and I involve desferrioxamine B (DFOB) as model siderophore, whereas desferrichrome (DFC) was used in batch F. Batches A and B were conducted as time-series experiments under anoxic conditions for ocean-island basalt BHVO-2 and granite GSAF3 and as 24 hr experiments for all other samples. Time intervals in anoxic batches A and B partially overlap as a mean to assess reproducibility. Experiments C, G and H are anoxic and hypoxic batches conducted independently of A and B also to evaluate reproducibility. The batches D and I are time-series experiments similar to A, but were conducted under hypoxic and oxic conditions, whereas E is a 24 hr experiment conducted under oxic conditions. Note that some of these are repetitions of the oxic experiments presented in Kraemer *et al.* (2015) and published data are shown for sample OL20-B for the oxic experiments due to insufficient amounts of sample powder left in the course of the experiments. Batch F consists of experiments conducted under anoxic, hypoxic and oxic conditions on ocean-island basalt BHVO-2 with the model siderophore DFC.

The experimental setup was modified after Kraemer *et al.* (2015). Except for BHVO-2 which is a certified reference material and issued already as rock powder by the United States Geological Survey, the rock samples were crushed, rinsed with DI and after drying ground with a Fritsch Pulverisette 6 planetary ball mill with agate mortar. Bulk decomposition of the powdered rock samples (including BHVO-2) was carried out using a Picotrace DAS acid digestion system (Pico Trace, Germany) following a mixed acid (HF-HNO_3-HCl) digestion protocol (Dulski, 2001). For the leaching experiments, the sample powders were gravimetrically weighed into acid-cleaned 50 to 250ml LDPE bottles matching a solid content of 20g/L. The batch leaching experiments were conducted in a trace metal-clean environment with acid-cleaned labware as follows:

Experiments conducted under oxic conditions
For the oxic experiments, the solutions were prepared and the experiments conducted under ambient conditions. De-ionised (DI) water was filled into acid-cleaned LDPE bottles at an appropriate amount. The siderophore desferrioxamine B (DFOB) was obtained in its mesylate form as the drug Desferal (Novartis AG) which consists of pure desferrioxamine-B mesylate and which is commonly used to treat acute and chronic iron overload (Bernhardt, 2007; Nick *et al.*, 2003). The purity of Desferal was checked by reagent blank measurements; trace-element concentrations in Desferal were found to be at least two orders of magnitude lower than the concentrations in our experiments. Desferrichrome was obtained as Fe-free powder ('Ferrichrome Iron-free from Ustilago sphaerogena'; CAS-No: 34787-28-5) from Sigma Aldrich. The DFOB or DFC powders were added to the DI water by gravimetrically weighing in appropriate amounts of the powders (matching a final molarity of 1 mmol/L DFOB/DFC), the bottle was closed and shaken to facilitate dissolution. The pH was measured separately in small plastic beakers to avoid potential contamination by the pH electrode.

Experiments conducted under hypoxic and anoxic conditions
The anoxic and hypoxic experiments were conducted completely inside an Anaerobic Chamber manufactured by Coy Laboratory Products (Grass Lake, Michigan, USA). For hypoxic conditions, an O_2 controller was used, which constantly measures the oxygen concentration in the chamber and either adds nitrogen gas or air to the chamber to reach the desired O_2 concentration. This operating mode can reach hypoxic levels down to 0.1 % O_2. For completely anoxic conditions, the chamber is first purged with N_2 until O_2 concentration approaches 0.1 %. Then the chamber is purged with a

hydrogen gas mix (5 % H_2, 95 % N_2; 'forming gas') until H_2 concentration in the chamber reaches at least 3 %. In presence of the palladium catalyst, the hydrogen reacts with the remaining oxygen inside the chamber and water molecules are formed. With this technique, anoxic conditions are achieved and can be kept constant by continuously adding forming gas at defined time intervals, so that the consumed H_2 is replenished, and anoxic conditions are maintained by ensuring that at least 3.5-4.5 % H_2 are in the atmosphere of the chamber. Note that the manufacturer of the chamber provides a working range of "0-5 ppmv O_2" to account for the accuracy of the oxygen probe and potential leakage. We emphasise that H_2 concentrations were kept high enough throughout the experiments so that any O_2 leakage into the chamber was minimised as good as possible and the O_2 probe actually showed readings of 0 ppmv throughout the whole experiments. Any O_2 leaking in would immediately be removed by reaction with H_2 to H_2O at the Pd catalyst. Leakage of ambient air into the chamber would also immediately be visible by sharply increasing humidity readings due to the H_2O formation in the chamber. However, these remained constant throughout the experiments.

Before the atmosphere was changed, all labware needed for the experiments was put inside the chamber to minimise contamination of the atmosphere with ambient air during the experiment, for example when the airlock is used. The chamber was sealed and purged with N_2 and forming gas to reach anoxic conditions of 0 ppmv as indicated by the oxygen probe inside the chamber. The bottle with DI water was opened and stirred with a magnetic stirrer for at least 12 hours at anoxic conditions in the anaerobic chamber to remove any dissolved oxygen from the solution. A multimeter with a free dissolved oxygen (FDO) probe was used to verify that the DI solution was free of dissolved oxygen (see Table S-2). For the anoxic experiments, the siderophore powder, which was weighed in into small plastic beakers under ambient conditions, was then added after equilibration with the solution and stirred for at least another hour. The FDO content was then verified again in separate aliquots. For the hypoxic experiments, the DI water was first stirred in a similar way under anoxic conditions until FDO reached 0.0 %. Then, some ambient air was added to the chamber to achieve and maintain an O_2 concentration of 0.1 % with the help of the O_2 controller. The DI solution was stirred for another 12 hours to equilibrate with the hypoxic atmosphere. Afterwards, the FDO was checked and DFOB or DFC were added to the solution. After stirring for at least another hour, FDO was verified again.

Apart from the procedures described above, all experiments followed the same protocol. The solutions containing exactly 1 mmol/L DFOB and 1 mmol/L DFC were added via graduated acid-cleaned plastic cylinders either inside (hypoxic, anoxic experiments) or outside (oxic experiments) of the chamber to the LDPE bottles containing the rock powders. The bottles were then closed and handshaken to facilitate suspension and put on an orbital shaker operated at 180 rpm. The bottles were covered with aluminium foil to minimise UV-induced decomposition of the organic ligands. After the designated time, the suspensions were filtered with acid-cleaned syringe filters with a membrane pore size of 0.2 µm into new acid-cleaned LDPE bottles. A ca. 1 ml aliquot was taken for the determination of pH before the remaining solution (ca. 24ml for the majority of the DFOB experiments, less for DFC experiments) was acidified with 1 ml HCl and 10 µl HF for stabilization. For the time-series experiments, 250 ml suspensions were used and 10 ml aliquots of the well-shaken sample were taken and filtered with a filter syringe at the desired time interval and the added amounts of HCl and HF were adapted. We emphasise that for the anoxic and hypoxic experiments, all described steps were conducted inside the chamber and that the oxygen concentrations, which were constantly monitored, remained at 0 ppmv throughout the anoxic and at 0.1 % O_2 during the hypoxic experiments. The solutions were only removed from the atmosphere after filtration and acidification. Solution pH was measured inside the chamber under hypoxic and anoxic conditions, respectively. After using the airlock or entering the chamber with the gloves, extra care was taken that O_2 concentrations reached 0 ppmv again before the start of any activities inside the chamber.

Control experiments without siderophores

In a previous study (Kraemer *et al.*, 2015), we indicated that 24 hr control experiments under oxic conditions without DFOB (only DI) were below the detection limit of the ICP-MS and demonstrated with control experiments with HCl and acetic acid that Ce anomaly formation only occurred in presence of the siderophore DFOB. Here, we conducted

additional control experiments with DI and 0.01 mol/L HCl (pH 2) under strictly anoxic conditions as laid out in the previous paragraph. The resulting REY_{BN} patterns are presented in Figure S-6. In contrast to the siderophore experiments, REY in the DI experiments were mostly below the detection limit after 5 min of leaching and after 24 hours of leaching detectable only in some experiments (MORB-TP cryst, MORB-TP glass, A-Jp, GSAF3). Neither the DI nor the HCl experiments produced any Ce_{BN} anomalies in the leachates.

Analytical & Reporting

All solutions were measured for their REY compositions with a Perkin Elmer NexION 350x ICP-MS coupled to an Apex 2 desolvating nebulizer by Elemental Scientific. Interference correction for the rare earth elements as employed in this study was modified after Dulski (1994).

REY patterns in the bulk rocks are shown as chondrite-normalised REY patterns (REY_{CN}). C1 chondrite data used for normalisation was obtained from Anders and Grevesse (1989). The REY concentrations in the leachates are normalised to the respective bulk rock REY concentrations (REY_{BN}) in order to illustrate the fractionation induced by siderophore leaching from the rock material.

Ce anomalies are reported as Ce_N/Ce_N^* (Eq. S-1, (Bau *et al.*, 1996)) and are calculated with C1-chondrite normalised values. As the bulk-rock REY patterns do not show any anomalous behaviour of Ce, the anomalies were calculated with chondrite-normalised values. The Ce_N/Ce_N* ratio is a measure of the anomalous behaviour of Ce, with values below unity indicating negative, values above unity indicating positive anomalies against the normalisation standard (here: chondrite).

Equation S-1:

$$\frac{Ce_N}{Ce_N^*} = \frac{Ce_N}{(0.5 * La_N + 0.5 * Pr_N)}$$

Supplementary Tables

Table S-1 Mineralogical composition of some of the rock samples (taken from Kraemer *et al.,* 2015). The samples BHVO-2 and BIRN-3 (not listed) are typical microcrystalline basalts with no visible secondary alteration. Abbreviations: Ol = olivine, Px = Pyroxene, Cpx = clinopyroxene, Mt = titanomagnetite, Plg = plagioclase.

Sample	Mineralogy	Reference
OIB-Me	*Ol* and *Cpx* phenocrysts in a glassy matrix of *Plg* and *Mt,* no visible secondary minerals	Giese and Bau (1994)
OIB-Haw	Phenocrysts of *Ol* in a matrix of *Plg*, *Cpx* and glass, no visible secondary minerals	Giese and Bau (1994)
MORB-EPR	*Ol*, *Plg* and *Px* microcrystallites in a partially devitrified glassy matrix, no visible secondary minerals	Giese and Bau (1994)
MORB-TP	Microcrystalline Ol, Plg and Px, no visible secondary minerals	Kraemer *et al.* (2015)
A-Jp	Microcrystalline *Plg*, *Cpx* and minor *Ol*, no visible secondary minerals	Bau (1998)
OL20B	Phenocrysts of *Plg* and *Cpx* in a *Px*-dominated matrix, minor amounts of sericite, chlorite and clay minerals indicate small-scale rock alteration	Schnurr (1995)
GSAF3	*Plg*, *Qtz*, minor mica, no secondary minerals	Kraemer *et al.* (2015)

Table S-2 Overview of the different experimental setups / runs. Times marked with an asterisk indicate that these experiments were only done with BHVO-2 and GSAF3 (as longer time-series experiments). The desferrichrome experiments (batch F) were only conducted with BHVO-2. FDO was determined with a multimeter probe after solution equilibration inside the chamber as described in the methods part of this article.

Experiment	Reagent	Experiment time	Solid content	Oxygen concentration in anaerobic chamber	Free dissolved oxygen (FDO) saturation in DFOB solution
A	1 mmol/L DFOB	5 min*, 1 hr*, 4 hr*, 8 hr*, 24 hr	20 g/L	0 ppmv O_2	0.0 %
B	1 mmol/L DFOB	5 min, 20 min*, 1 hr	20 g/L	0 ppmv O_2	0.0 %
C	1 mmol/L DFOB	24 hr	20 g/L	0 ppmv O_2	0.0 %
D	1 mmol/L DFOB	5 min*, 1 hr*, 4 hr*, 8 hr*, 24 hr	20 g/L	0.1 % O_2	1.5 %
E	1 mmol/L DFOB	24 hr	20 g/L	21 % O_2 (PAL)	100 %
F	1 mmol/L DFC	5 min, 24 hr	20 g/L	0 ppmv O_2 0.1 % O_2 21 % O_2 (PAL)	0.0 % 1.4 % 100 %
G	1 mmol/L DFOB	5 min, 24 hr	20 g/L	0 ppmv O_2	0.0 %
H	1 mmol/L DFOB	5 min, 24 hr	20 g/L	0.1 % O_2	1.4 %
I	1 mmol/L DFOB	5 min*, 1 hr*, 4 hr*, 8 hr*, 24 hr*, 144 hr*	20 g/L	21 % O_2 (PAL)	100 %

Table S-3 Bulk rock REY compositions of the igneous rocks used for leaching experiments, obtained from Kraemer *et al.*, 2015; except for BHVO-2 and BIRN3 (this study). All reported concentrations are in mg kg^{-1}.

Type	Mid-ocean ridge basalt	Mid-ocean ridge basalt	Ocean island tholeitic basalt	Ocean island tholeitic basalt	Ocean island alkali basalt	Ocean-island basalt	Basaltic andesite	Island-arc andesite	Granite
Locality	Atlantic Ridge Turtle Pit	Atlantic Ridge, Turtle Pit	Hawaii, Pacific Ocean	Hawaii, Pacific Ocean	Mehetia Island, Pacific Ocean	Dingle, Ireland	South Africa	Hokkaido, Japan	Bushveld, South Africa
Sample name	**MORB-TP**	**MORB-TP glass**	**BHVO-2**	**OIB-Haw**	**OIB-Me**	**BIRN3**	**OL-20B**	**A-Jp**	**GSAF3**
La	2.92	2.96	15.50	11.47	41.15	12.50	19.10	4.55	67.36
Ce	8.69	8.87	38.10	28.56	89.60	29.60	37.60	10.50	147.35
Pr	1.48	1.51	5.59	4.18	11.45	3.81	4.32	1.48	17.61
Nd	8.10	8.19	24.50	19.85	48.87	16.17	16.80	6.86	60.16
Sm	2.77	2.83	6.00	5.28	10.52	4.57	3.35	1.87	16.44
Eu	1.08	1.10	2.10	1.86	3.23	1.37	1.01	0.68	0.38
Gd	3.86	3.88	6.60	5.75	9.46	5.48	3.25	2.26	18.79
Tb	0.67	0.68	0.94	0.88	1.29	0.89	0.51	0.37	3.73
Dy	4.49	4.61	5.40	5.16	6.43	5.91	3.16	2.46	26.25
Y	25.80	26.10	25.30	24.26	27.00	33.60	18.00	13.94	160.70
Ho	0.96	0.98	0.98	0.97	1.06	1.16	0.67	0.54	5.41
Er	2.81	2.86	2.55	2.54	2.49	3.61	1.93	1.56	16.43
Tm	0.40	0.41	0.34	0.33	0.29	0.46	0.28	0.22	2.15
Yb	2.58	2.64	2.10	1.97	1.59	3.49	1.88	1.56	15.46
Lu	0.39	0.39	0.28	0.29	0.22	0.55	0.29	0.23	2.22
Ratios									
Y/Ho	26.79	26.63	25.82	25.01	25.47	28.97	26.91	25.81	29.70
Ce_{CN}/Ce_{CN}^{*}	0.99	1.00	1.02	0.99	0.98	1.02	0.96	0.97	1.01

Table S-4 Data Table with leachate concentrations, calculated Ce anomalies, Y-Ho ratios and pH of the siderophore experiments.

Table S-4 is available for download as an Excel file in the online version of this article at https://doi.org/10.7185/geochemlet.2227.

Supplementary Figures

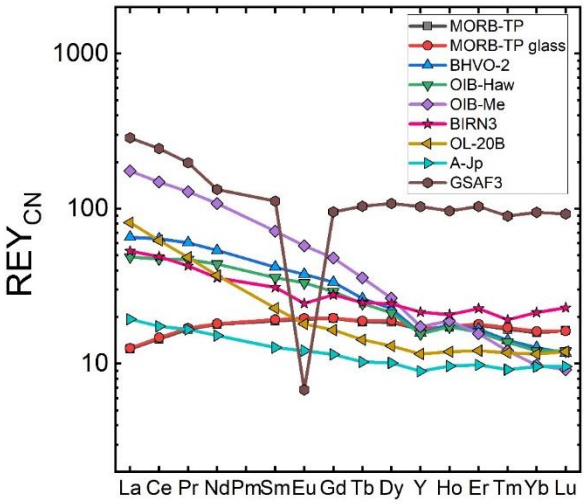

Figure S-1 Chondrite-normalised REY patterns of the bulk rock samples used for the leaching experiments. Note the absence of Ce_{CN} anomalies in all rock samples which could bias the bulk-rock normalised REY patterns of the leachates.

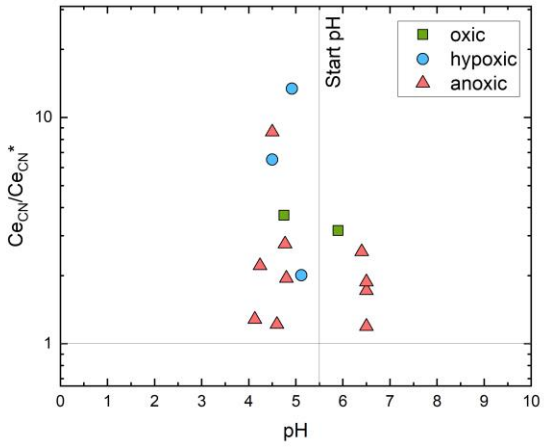

Figure S-2 Leachate pH versus Ce anomaly (expressed as Ce_{CN}/Ce_{CN}^*) of the leachates after 5 min of leaching in presence of siderophores.

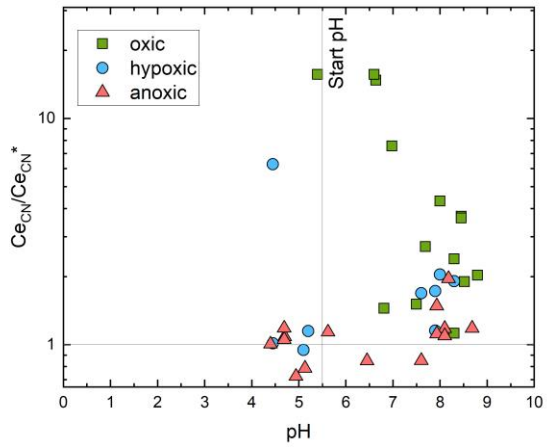

Figure S-3 Leachate pH versus Ce anomaly (expressed as Ce_{CN}/Ce_{CN}^*) of the leachates after 24 hours of leaching in presence of siderohores.

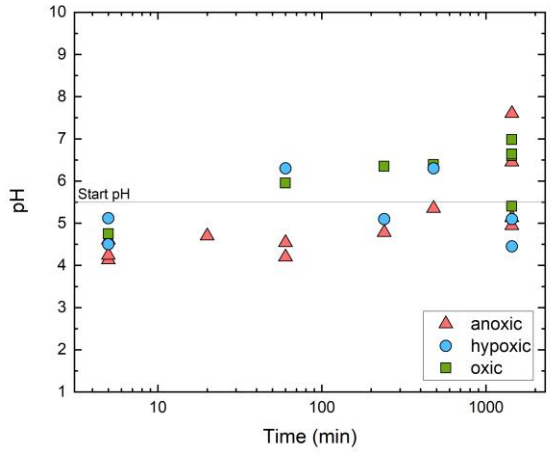

Figure S-4 pH versus time for the BHVO-2 siderophore experiments conducted under anoxic, hypoxic and oxic conditions.

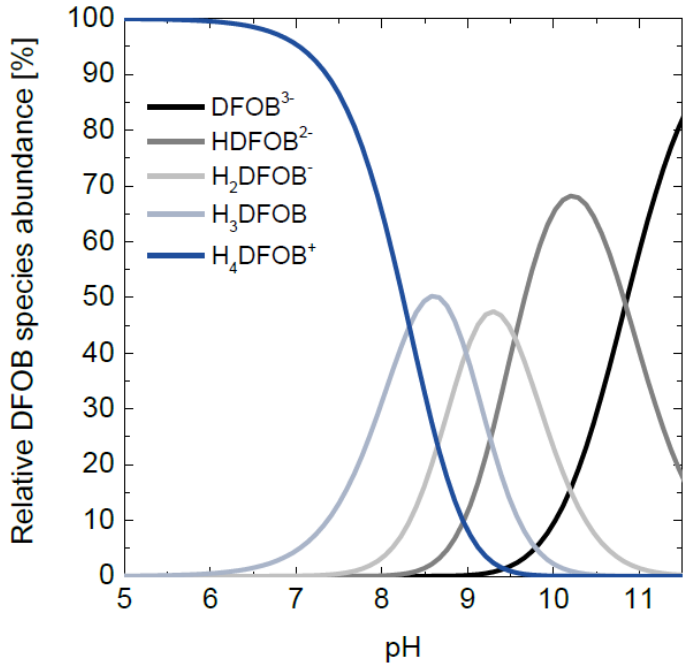

Figure S-5 Speciation curves for DFOB as calculated by HySS2009 modelling using constants of Martell and Smith (2001; I = 0.1, T = 25 °C).

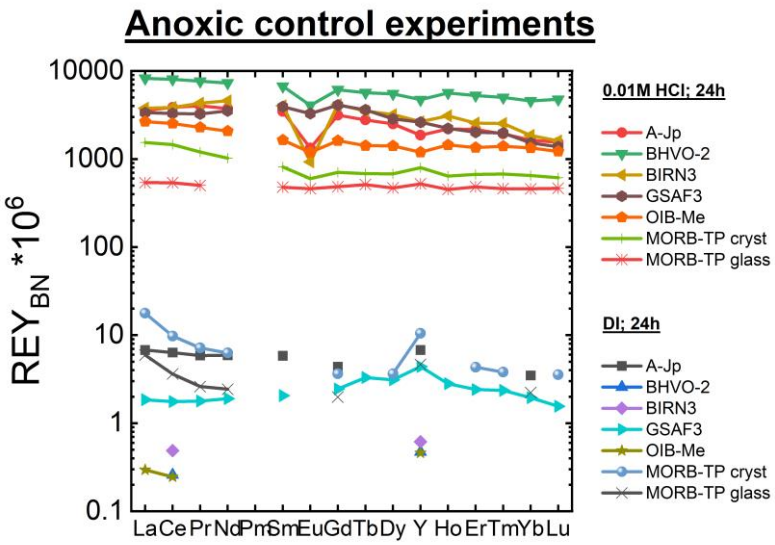

Figure S-6 Bulk rock-normalised REY patterns of control experiments (with DI and 0.01M HCl) conducted under anoxic conditions. Note the absence of Ce anomalies in all control experiments. Leachate REY concentrations for short-term DI leaching (<60 min) were below the detection limit and are not shown.

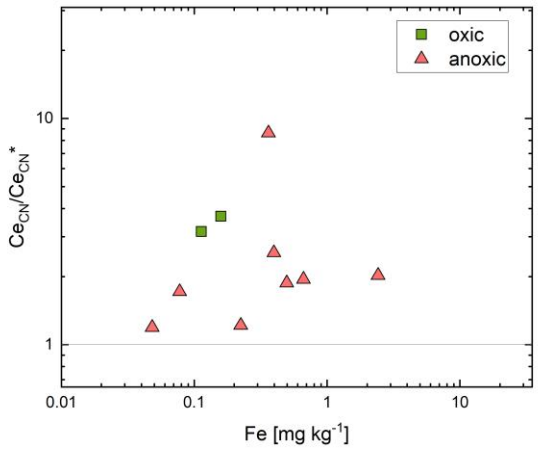

Figure S-7 Leachate Fe concentrations versus Ce anomaly (expressed as Ce_{CN}/Ce_{CN}^*) after 5 min of leaching with siderophores.

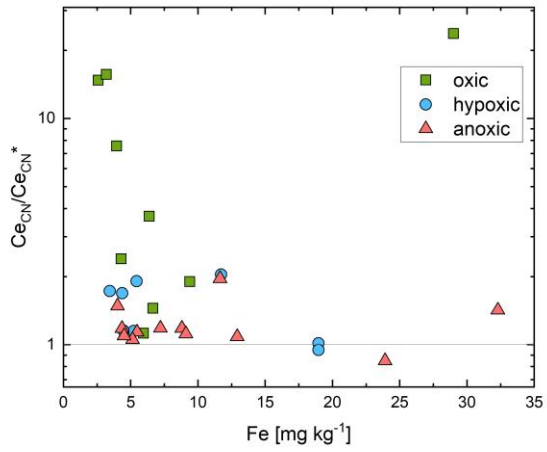

Figure S-8 Leachate Fe concentrations *versus* Ce anomaly (expressed as Ce_{CN}/Ce_{CN}^*) after 24 hours of leaching with siderophores.

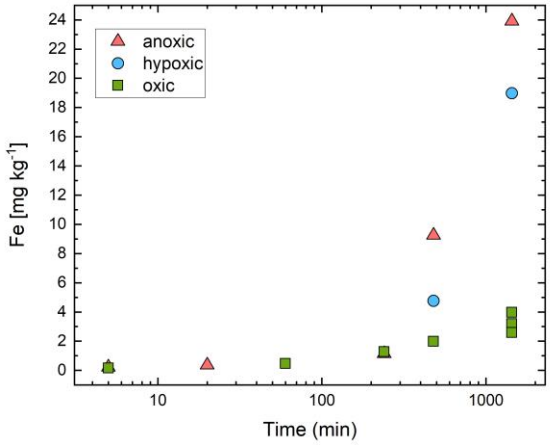

Figure S-9 Leachate Fe concentrations (in mg/kg) *versus* time for the BHVO-2 siderophore experiments conducted under anoxic, hypoxic and oxic conditions.

Supplementary Information References

Anders, E., Grevesse, N. (1989) Abundances of the elements: Meteoritic and solar. *Geochimica et Cosmochimica Acta* 53, 197–214. https://doi.org/10.1016/0016-7037(89)90286-X

Bau, M., Koschinsky, A., Dulski, P., Hein, J.R. (1996) Comparison of the partitioning behaviours of yttrium, rare earth elements, and titanium between hydrogenetic marine ferromanganese crusts and seawater. *Geochimica et Cosmochimica Acta* 60, 1709–1725. https://doi.org/10.1016/0016-7037(96)00063-4

Bau, M., Usui, A., Pracejus, B., Mita, N., Kanai, Y., Irber, W., Dulski, P. (1998) Geochemistry of low-temperature water-rock interaction: Evidence from natural waters, andesite, and iron-oxyhydroxide precipitates at Nishiki-numa iron-spring, Hokkaido, Japan. *Chemical Geology* 151, 293–307. https://doi.org/10.1016/S0009-2541(98)00086-2

Bernhardt, P.V. (2007) Coordination chemistry and biology of chelators for the treatment of iron overload disorders. *Dalton Transactions* 30, 3214–3220. https://doi.org/10.1039/b708133b

Binard, N., Maury, R.C., Guille, G., Talandier, J., Gillot, P.Y., Cotten, J. (1993) Mehetia Island, South Pacific: geology and petrology of the emerged part of the Society hot spot. *Journal of Volcanology and Geothermal Research* 55, 239–260. https://doi.org/10.1016/0377-0273(93)90040-X

Dulski, P. (1994) Interferences of oxide, hydroxide and chloride analyte species in the determination of rare earth elements in geological samples by inductively coupled plasma-mass spectrometry. *Fresenius' Journal of Analytical Chemistry* 350, 194–203. https://doi.org/10.1007/BF00322470

Dulski, P. (2001) Reference Materials for Geochemical Studies: New Analytical Data by ICP-MS and Critical Discussion of Reference Values. *Geostandards Newsletter* 25, 87–125. https://doi.org/10.1111/j.1751-908X.2001.tb00790.x

Giese, U., Bau, M. (1994) Trace element accessibility in mid-ocean ridge and ocean island basalt: an experimental approach. *Mineralogical Magazine* 58A, 329–330. https://doi.org/10.1180/minmag.1994.58A.1.173

Haase, K.M., Petersen, S., Koschinsky, A., Seifert, R., Devey, C. W., Keir, R., Lackschewitz, K.S., Melchert, B., Perner, M., Schmale, O., Süling, J., Dubilier, N., Zielinski, F., Fretzdorff, S., Garbe-SchöNberg, D., WesternströEr, U., German, C.R., Shank, T.M., Yoerger, D., Giere, O., Kuever, J., Marbler, H., Mawick, J., Mertens, C., Stöber, U., Walter, M., Ostertag-Henning, C., Paulick, H., Peters, M., Strauss, H., Sander, S., Stecher, J., Warmuth, M., Weber, S. (2007) Young volcanism and related hydrothermal activity at 5°S on the slow-spreading southern Mid-Atlantic Ridge. *Geochemistry, Geophysics, Geosystems* 8. https://doi.org/10.1029/2006GC001509

Kraemer, D., Kopf, S., Bau, M. (2015) Oxidative mobilization of cerium and uranium and enhanced release of "immobile" high field strength elements from igneous rocks in the presence of the biogenic siderophore desferrioxamine B. *Geochimica et Cosmochimica Acta* 165, 263–279. https://doi.org/10.1016/j.gca.2015.05.046

Martell, A., Smith, R. (2001) *NIST Stability Constants of Metal Complexes Database 46, 6.0*. Gaithersburg, MD.

Nick, H., Acklin, P., Lattmann, R., Buehlmayer, P., Hauffe, S., Schupp, J., Alberti, D. (2003) Development of Tridentate Iron Chelators: From Desferrithiocin to ICL670. *Current Medicinal Chemistry* 10, 1065–1076. https://doi.org/10.2174/0929867033457610

Schnurr, W. (1995) Spurenelementgeochemie proterozoischer Cherts, Jasper and Jaspilite der Ongeluk Lava und der basalen Hotazel Formation, Kaapvaal Kraton, Südafrika. Diploma Thesis, RWTH Aachen.